

MODELING OF TURBINE ENGINE AXIAL-FLOW COMPRESSOR AND TURBINE CHARACTERISTICS

M. O R K I S Z and S. S T A W A R Z (RZESZÓW)

The paper describes the concept of modeling the turbine engine axial-flow compressor and turbine characteristics by using the functions of two variables. Accuracy of the proposed concept has been verified on the example of the given compressor and turbine characteristics. Good agreement between the modeling results and experimental characteristics has been achieved.

1. INTRODUCTION

An aircraft gas turbine engine represents a complex system where performance and component matching depend on the flight parameters, design and operational conditions (e.g., the variation in tip blade clearance or the degree of pollution of the surface of elements in the main duct of the compressor). The majority of problems in developing an adequate gas turbine simulation model are related to inaccuracies in the prediction of the component characteristics, especially for the compressor and turbine. A review of the available simulation models presented in the literature indicate that computer models usually require the functional forms of the compressor and turbine characteristics given below:

$$(1.1) \quad \begin{aligned} \dot{m}_{zr} &= f_1(n_{zr}, \pi_S^*), & \eta_S^* &= f_2(n_{zr}, \pi_S^*), \\ \pi_T^* &= f_3(n'_{zr}, \dot{m}'_{zr}), & \eta_T^* &= f_4(n'_{zr}, \pi_T^*), \end{aligned}$$

where \dot{m}_{zr} – corrected mass flow of air; \dot{m}'_{zr} – corrected mass flow of combustion gases; n_{zr} – corrected rotational speed of compressor; n'_{zr} – corrected rotational speed of turbine; π_S^* – compressor pressure ratio; π_T^* – turbine expansion ratio; η_S^* – isentropic compressor efficiency; η_T^* – isentropic turbine efficiency.

Simulation analysis of the influence of some of the above described parameters can be explored numerically. That can be realized on the basis of available experimental compressor and turbine performance map (see Figs. 1 and 2).

For digital modeling, as in the designing process, it is most important to preserve the minimum discrepancy between the original data values, usually given in form of charts (e.g., compressor or turbine performance characteristics),

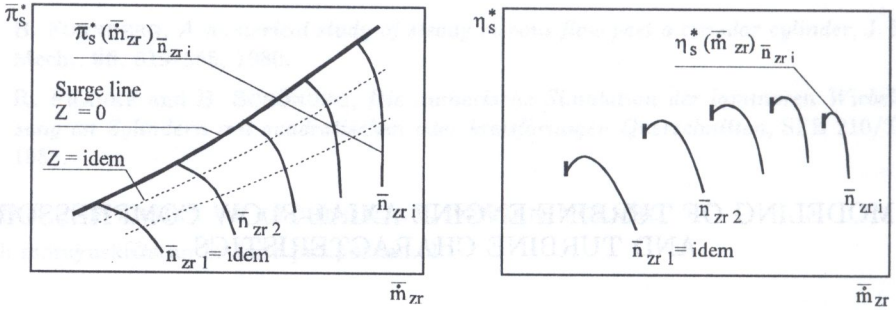


FIG. 1. Example of compressor performance map.

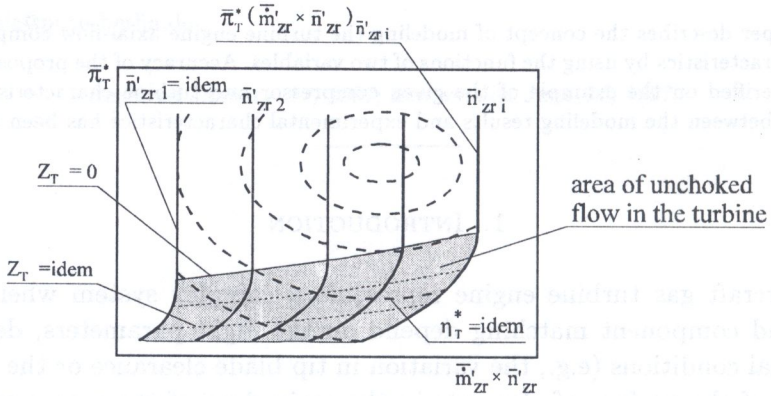


FIG. 2. Example of turbine performance map.

and their predicted values. Focusing the attention on the modeling problems with compressor and turbine characteristics, let us mention several potential sources of troubles. These are (EL-GAMMAL [3]):

- 1) Determination of the shape of characteristics (see Figs. 1, 2, 3 and 4).
- 2) The nonuniqueness problem.
- 3) The ill-conditioning problem, where some small changes in the variable of one coordinate produce large changes in the other coordinate variables.
- 4) The large variation encountered in the variables if the full envelope compressor or turbine characteristics is desired.
- 5) The differences in the order of magnitude of variables (scaling problem).

A review of the published papers on this subject shows that there is still a need for a general solution that can be used to model the compressor and turbine performance map. DOBRANSKI and MARTIANOWA [1] used the look-up tables to store the characteristics and linear or Lagrangian interpolation technique to determine the values of the performance parameters for an arbitrarily selected point on the performance map. Similar technique was also applied by ISMAIL and BHINDER [2]. It is important to note that for an adequate estimation of the

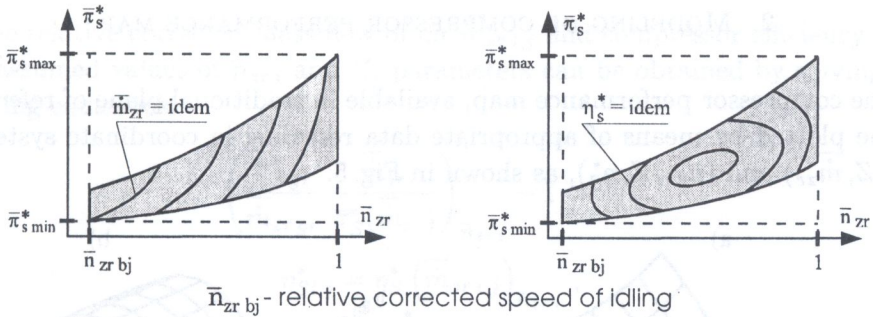


FIG. 3. Compressor contour maps of relative corrected mass flow \bar{m}_{zr}^* , and efficiency η_s^* .

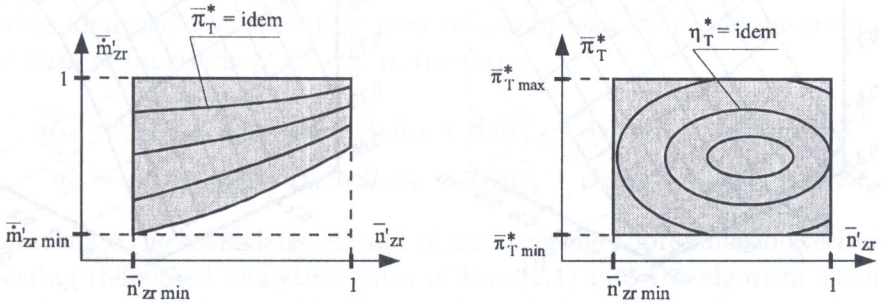


FIG. 4. Turbine contour maps of relative expansion ratio $\bar{\pi}_T^*$ and efficiency η_T^* .

characteristics, the interpolation algorithm requires a quite narrow calculation step in order to assure the proper variation of parameters. The error limits for the mentioned models are guaranteed in original data points, while the error in intermediate points usually suffer unreal fluctuations. In order to obtain better model outputs, EL-GAMMAL [3] developed the criteria and algorithm for compressor characteristics real-time model and approximation. This method allows to choose objectively the most adequate model according to known performance data. Moreover, the analysis of the monotonic behavior of the given data and data rescaling is necessary. The rational functions and an elliptic approximation introduced by HORMOUZIADIS and HERBIG [4] to describe the speed curves and efficiency contours on compressor performance map cover also the various aspects of modeling the compressor characteristics.

The aim of this study is to describe a certain concept of modeling the compressor and turbine characteristics that has been developed especially for digital simulation of the transient-state operation of gas turbine engines. This concept requires the two-variable functions and data rescaling. In addition, this concept can be used to represent either a part or full envelope of characteristics, without the usually encountered limits.

2. MODELING OF COMPRESSOR PERFORMANCE MAP

The compressor performance map, available in traditional plane of reference, can be plotted by means of appropriate data rescaling in coordinate system of $(\bar{n}_{zr}, Z, \dot{m}_{zr})$ and $(\bar{n}_{zr}, Z, \eta_s^*)$, as shown in Fig. 5.

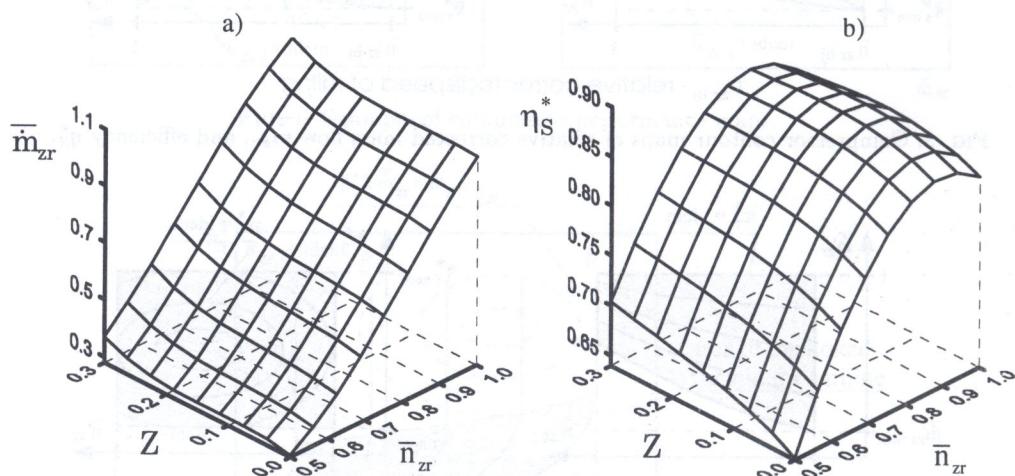


FIG. 5. Graphical representation of functions: a) $\bar{m}_{zr} = f_5(\bar{n}_{zr}, Z)$, b) $\eta_s^* = f_6(\bar{n}_{zr}, Z)$ for K-15 compressor performance map.

For the new characteristics:

$$(2.1) \quad \bar{m}_{zr} = f_5(\bar{n}_{zr}, Z), \quad \eta_s^* = f_6(\bar{n}_{zr}, Z),$$

where Z is the coefficient of relative stability margin of the compressor, it is possible to achieve a good fit by means of the interpolation or approximation technique, without the limits as previously introduced. Before finding the analytical expression of functions (2.1), it is necessary to store the compressor characteristic in tables. The form of these tables is shown below (Tables 1 and 2).

Table 1. Mass flow vs coefficient of relative stability margin.

\bar{n}_{zr}	$\bar{n}_{zr i}$
Z	\vdots
Z_j	$\bar{m}_{zr i, j}$

Table 2. Compressor efficiency vs the coefficient of relative stability margin.

\bar{n}_{zr}	$\bar{n}_{zr i}$
Z	\vdots
Z_j	$\eta_{s i, j}$

The relative corrected mass flow of air $\bar{m}_{zr i,j}$ and compressor efficiency $\eta_{S i,j}^*$ with assumed values of $\bar{n}_{zr i}$ and Z_j parameters can be obtained by solving the following equations:

$$(2.2) \quad \left(\frac{\bar{\pi}_{S gr}^* \bar{m}_{zr}}{\bar{m}_{zr gr} \bar{\pi}_S^*(\bar{m}_{zr})} \right)_{\bar{n}_{zr i}} - 1 = Z_j,$$

$$\eta_{S i,j}^* = \eta_S^* \left(\bar{m}_{zr i,j} \right)_{\bar{n}_{zr i}},$$

where $\bar{\pi}_S^*(\bar{m}_{zr})$, $\eta_S^*(\bar{m}_{zr})$ – fitting function of $\bar{n}_{zr i}$ curve (see Fig. 1); $\bar{\pi}_{S gr}^*$, $\bar{m}_{zr gr}$ – surge line relative pressure ratio and corrected mass flow, respectively.

Having analyzed the operating area of compressor map and assuming the generic form of functions (2.1), e.g. in the form

$$(2.3) \quad \bar{m}_{zr} = f_3(\bar{n}_{zr}, Z) = A_0 + A_1 \bar{n}_{zr} + A_2 \bar{n}_{zr}^2 + A_3 \bar{n}_{zr} Z + A_4 Z + A_5 Z^2,$$

$$\eta_S^* = f_4(\bar{n}_{zr}, Z) = B_0 + B_1 \bar{n}_{zr} + B_2 \bar{n}_{zr}^2 + B_3 \bar{n}_{zr} Z + B_4 Z + B_5 Z^2,$$

we can estimate the coefficients A_i and B_i by using the approximation technique.

Inserting the closed analytical form of Eqs. (2.1) into the algorithm as shown in Fig. 6, we can finally establish an analytical description of the compressor map. For the surge line modeling, the pressure ratio $\bar{\pi}_{S gr}^*$ and corrected mass flow $\bar{m}_{zr gr}$ as functions of the corrected rotational speed \bar{n}_{zr} of the rotor are requested.

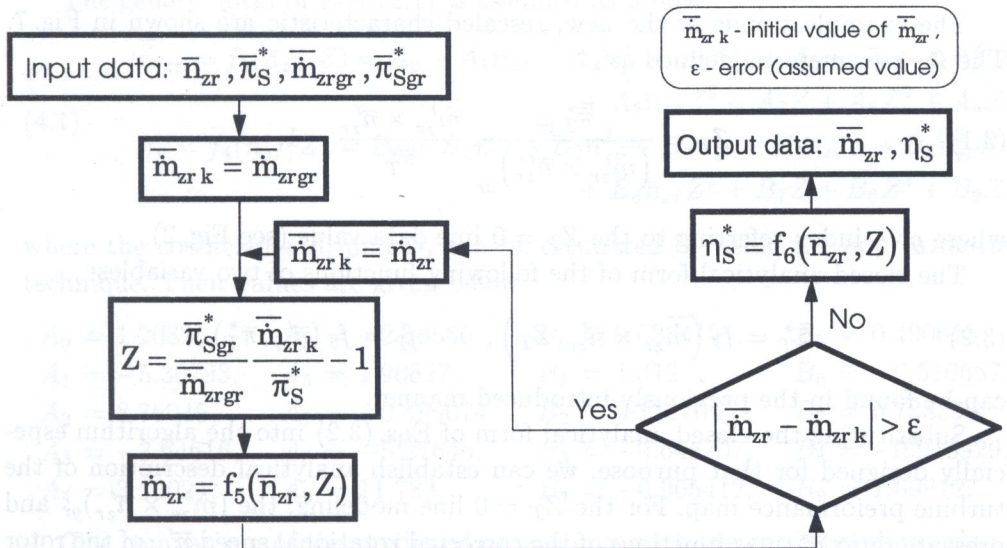


FIG. 6. Flow diagram (model of compressor performance map).

3. MODELING OF TURBINE PERFORMANCE MAP

As in the case of the compressor, a similar technique can be also applied to describe the behavior of the turbine performance data. The turbine performance characteristics usually plotted as shown in Fig. 2, after some manipulations can be presented in other coordinate systems of $(\overline{m}'_{zr} \times \overline{n}'_{zr}, Z_T, \overline{\pi}_T^*)$ and $(\overline{n}'_{zr}, \overline{\pi}_T^*, \eta_T^*)$.

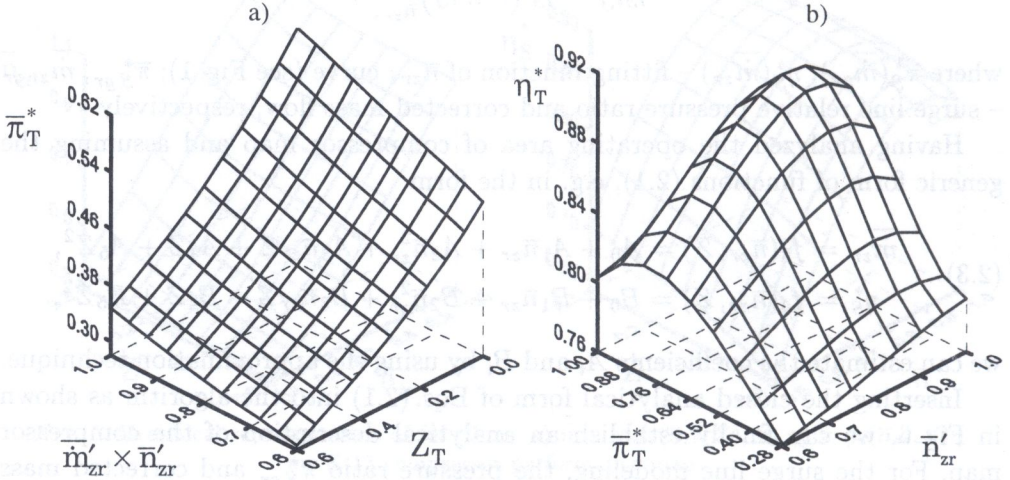


FIG. 7. Graphical representation of functions: a) $\overline{\pi}_T^* = f_7(\overline{m}'_{zr} \times \overline{n}'_{zr}, Z_T)$,
b) $\eta_T^* = f_8(\overline{n}'_{zr}, \overline{\pi}_T^*)$.

The example trends of the new, rescaled characteristic are shown in Fig. 7. The Z_T parameter is defined as

$$(3.1) \quad Z_T = \frac{\overline{\pi}_T^*{}_{gr}}{(\overline{m}'_{zr} \times \overline{n}'_{zr})_{gr}} \frac{\overline{m}'_{zr} \times \overline{n}'_{zr}}{\overline{\pi}_T^*} - 1,$$

where gr - index referring to the $Z_T = 0$ line data value (see Fig. 2).

The closed analytical form of the following functions of two variables:

$$(3.2) \quad \overline{\pi}_T^* = f_7(\overline{m}'_{zr} \times \overline{n}'_{zr}, Z_T), \quad \eta_T^* = f_8(\overline{n}'_{zr}, \overline{\pi}_T^*),$$

can be found in the previously introduced manner.

Substituting the closed analytical form of Eqs. (3.2) into the algorithm especially designed for that purpose, we can establish analytical description of the turbine performance map. For the $Z_T = 0$ line modeling, the $(\overline{m}'_{zr} \times \overline{n}'_{zr})_{gr}$ and pressure ratio $\overline{\pi}_T^*{}_{gr}$ as functions of the corrected rotational speed \overline{n}'_{zr} of the rotor are requested. The algorithm is presented in Fig. 8.

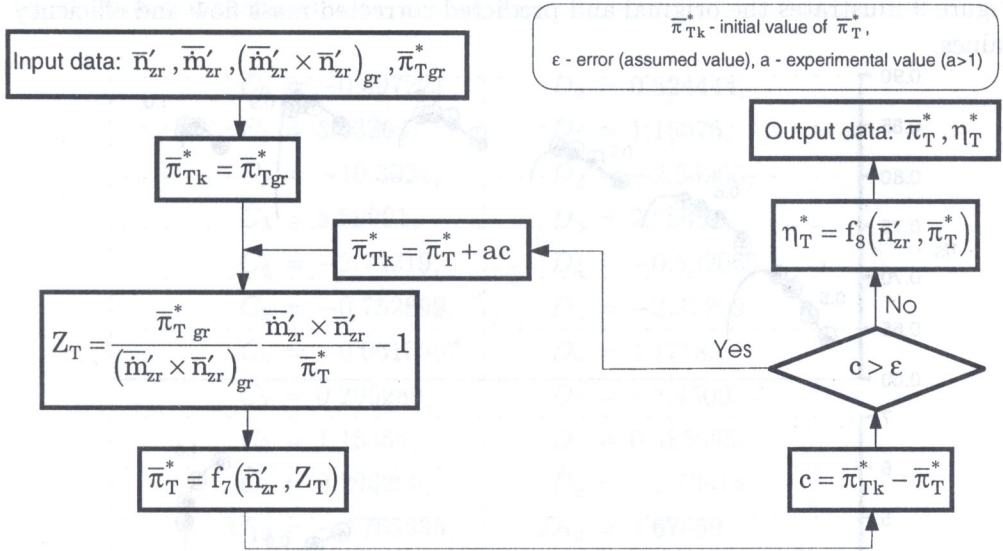


FIG. 8. Flow diagram (model of turbine performance map).

4. CALCULATIONS

In order to verify the accuracy of the described modeling concept, the example of compressor and turbine characteristics has been considered. In the case of the compressor characteristic, the range of parameters $\bar{n}_{zr} = 0.5 \div 1$ and $Z = 0 \div 0.3$ has been assumed, with the same size step equal to 0.1.

The generic form of Eqs. (2.1) is assumed as follows:

$$\begin{aligned}
 \bar{m}_{zr} &= f_3(\bar{n}_{zr}, Z) = A_0 + A_1 \bar{n}_{zr} + A_2 \bar{n}_{zr}^2 + A_3 \bar{n}_{zr}^3 + A_4 \bar{n}_{zr} Z + A_5 \bar{n}_{zr}^2 Z \\
 &\quad + A_6 \bar{n}_{zr} Z^2 + A_7 Z + A_8 Z^2 + A_9 Z^3, \\
 \eta_S^* &= f_4(\bar{n}_{zr}, Z) = B_0 + B_1 \bar{n}_{zr} + B_2 \bar{n}_{zr}^2 + B_3 \bar{n}_{zr}^3 + B_4 \bar{n}_{zr} Z + B_5 \bar{n}_{zr}^2 Z \\
 &\quad + B_6 \bar{n}_{zr} Z^2 + B_7 Z + B_8 Z^2 + B_9 Z^3,
 \end{aligned}
 \tag{4.1}$$

where the coefficients A_i and B_i can be estimated by using the approximation technique. Their values are given below:

$$\begin{array}{llll}
 A_0 = 1.20825, & A_5 = -2.56566, & B_0 = 0.0334191, & B_5 = 0.490655, \\
 A_1 = -5.30793, & A_6 = 1.90627, & B_1 = 1.31222, & B_6 = -0.510657, \\
 A_2 = 8.76045, & A_7 = -0.499074, & B_2 = 0.132704, & B_7 = 0.733399, \\
 A_3 = -3.64616, & A_8 = -5.27646, & B_3 = -0.646707, & B_8 = -0.910929, \\
 A_4 = 3.30021, & A_9 = 11.783, & B_4 = -0.905412, & B_9 = 1.69912.
 \end{array}$$

The comparison of the predicted data points with the corresponding original points, results in maximum error $\leq 1.5\%$ for corrected mass flow and efficiency.

Figure 9 illustrates the original and predicted corrected mass flow and efficiency values.

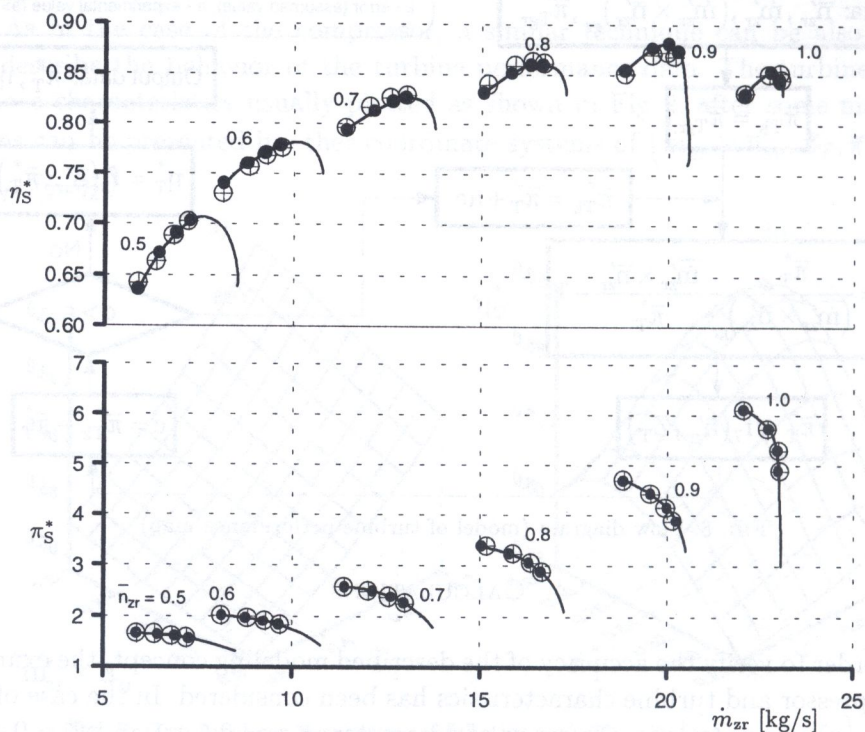


FIG. 9. Original (●) and the corresponding predicted (⊕) corrected mass flow and compressor efficiency.

The example of turbine performance map, like that of a compressor, has been considered at the range of $\bar{m}'_{zr} \times \bar{n}'_{zr} = 0.6 \div 1$ and $Z_T = 0 \div 0.6$, with the same size step equal to 0.1.

The generic form of Eqs. (3.2) is assumed as follows:

$$\begin{aligned}
 \bar{\pi}_T^* &= f_3(\bar{m}'_{zr} \times \bar{n}'_{zr}, Z_T) = C_0 + C_1(\bar{m}'_{zr} \times \bar{n}'_{zr}) + C_2(\bar{m}'_{zr} \times \bar{n}'_{zr})^2 \\
 &\quad + C_3(\bar{m}'_{zr} \times \bar{n}'_{zr})^3 + C_4(\bar{m}'_{zr} \times \bar{n}'_{zr})^4 + C_5(\bar{m}'_{zr} \times \bar{n}'_{zr}) Z_T \\
 &\quad + C_6(\bar{m}'_{zr} \times \bar{n}'_{zr})^2 Z_T + C_7(\bar{m}'_{zr} \times \bar{n}'_{zr})^3 Z_T + C_8(\bar{m}'_{zr} \times \bar{n}'_{zr}) Z_T^2 \\
 &\quad + C_9(\bar{m}'_{zr} \times \bar{n}'_{zr}) Z_T^3 + C_{10}(\bar{m}'_{zr} \times \bar{n}'_{zr})^2 Z_T^2 \\
 &\quad + C_{11} Z_T + C_{12} Z_T^2 + C_{13} Z_T^3 + C_{14} Z_T^4, \\
 \eta_T^* &= f_3(\bar{n}'_{zr}, \bar{\pi}_T^*) = D_0 + D_1 \bar{n}'_{zr} + D_2 \bar{n}'_{zr}{}^2 + D_3 \bar{n}'_{zr}{}^3 + D_4 \bar{n}'_{zr}{}^4 + D_5 \bar{n}'_{zr} \bar{\pi}_T^* \\
 &\quad + D_6 \bar{n}'_{zr}{}^2 \bar{\pi}_T^* + D_7 \bar{n}'_{zr}{}^3 \bar{\pi}_T^* + D_8 \bar{n}'_{zr} \bar{\pi}_T^{*2} + D_9 \bar{n}'_{zr} \bar{\pi}_T^{*3} + D_{10} \bar{n}'_{zr}{}^2 \bar{\pi}_T^{*2} \\
 &\quad + D_{11} \bar{\pi}_T^* + D_{12} \bar{\pi}_T^{*2} + D_{13} \bar{\pi}_T^{*3} + D_{14} \bar{\pi}_T^{*4},
 \end{aligned}
 \tag{4.2}$$

where values of coefficients C_i and D_i are:

$C_0 = -0.697221$	$D_0 = 0.524444,$
$C_1 = 5.63264,$	$D_1 = 1.15076,$
$C_2 = -10.3021,$	$D_2 = -2.53005,$
$C_3 = 8.69991,$	$D_3 = 2.28657,$
$C_4 = -2.72219,$	$D_4 = -0.522065,$
$C_5 = -0.752899,$	$D_5 = -2.37209,$
$C_6 = -0.0610567,$	$D_6 = 4.17183,$
$C_7 = 0.296289,$	$D_7 = -3.4509,$
$C_8 = 1.15354,$	$D_8 = 0.485065,$
$C_9 = 0.296296,$	$D_9 = -2.70615,$
$C_{10} = -0.765936,$	$D_{10} = 2.67659,$
$C_{11} = -0.105232,$	$D_{11} = 0.703948,$
$C_{12} = -0.0512211,$	$D_{12} = -0.90139,$
$C_{13} = -0.276549,$	$D_{13} = 1.3087,$
$C_{14} = -0.117051,$	$D_{14} = -0.00288276.$

The predicted data points compared with the corresponding original points give the maximum error $\leq 2.0\%$ for the expansion ratio and efficiency. Figure 10 illustrates the original and predicted expansion ratio, while Fig. 11 shows the original and predicted efficiency values.

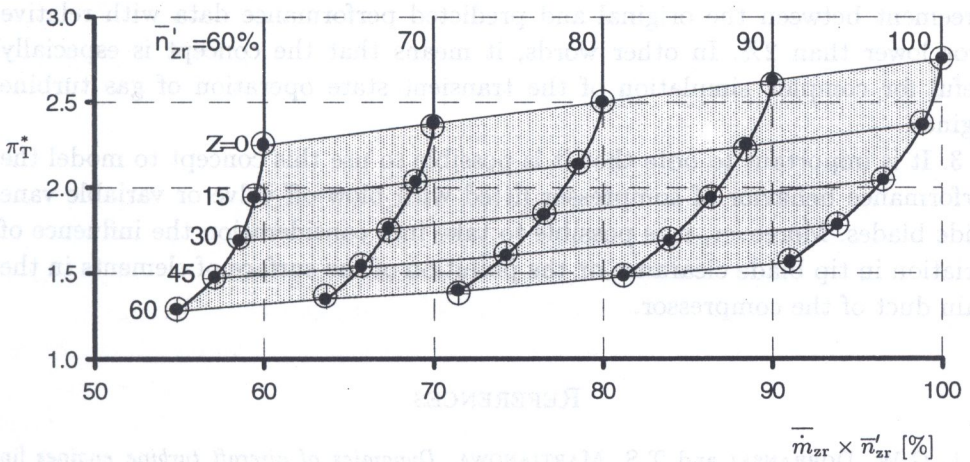


FIG. 10. Original (•) and the corresponding predicted (⊕) turbine expansion ratio.

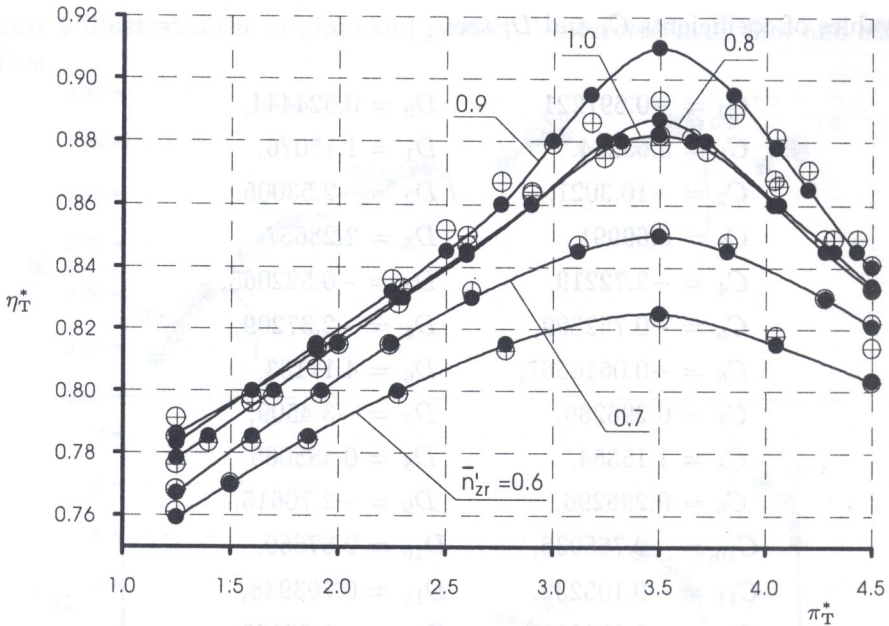


FIG. 11. Original (●) and the corresponding predicted (⊕) turbine efficiency.

5. CONCLUSIONS

1. The paper describes a concept used to model the compressor and turbine performance maps.

2. The presented concept is easy in use and enables us to model either a part or the entire area of characteristics. The example of calculation performed for K-15 compressor performance map and some turbine performance map show good agreement between the original and predicted performance data with relative error lower than 2%. In other words, it means that the concept is especially useful for complex simulation of the transient state operation of gas turbine engines.

3. It is important to note that it is possible to use this concept to model the performance behavior of compressor fitted with blow-off valve or variable vane guide blades. Moreover, it is possible to take into consideration the influence of variation in tip blade clearance or the pollution of the surface of elements in the main duct of the compressor.

REFERENCES

1. G.W. DOBRANSKI and T.S. MARTIANOWA, *Dynamics of aircraft turbine engines* [in Russian], Mashinostroenie, Moskva 1989.

2. I.H. ISMAIL and F.S. BHINDER, *Simulation of aircraft gas turbine engine*, J. Engng. for Gas Turbines and Power, Transactions of the ASME, Vol. 113, New York 1991, pp. 95-99.
3. M.A. EL-GAMMAL, *An algorithm and criteria for compressor characteristics real time modeling and approximation*, J. Engng. for Gas Turbines and Power, Transactions of the ASME, Vol. 113, New York 1991, pp. 112-117.
4. J. HORMOUZIADIS and H. HERBIG, *Numerische Simulation der Kennfelder von Strömungsmaschinen*, Konstruktion, pp. 182-186, 26, 1974.

DEPARTMENT OF AIRCRAFT ENGINES
RZESZÓW UNIVERSITY OF TECHNOLOGY.

Received March 7, 1997.